

# Comparison of the coseismic rupture with the aftershock distribution in the Hyuga-nada earthquakes of 1996

Yuji Yagi, Masayuki Kikuchi and Shingo Yoshida

Earthquake Research Institute, The University of Tokyo, Tokyo, Japan

Takeshi Sagiya

Geographical Survey Institute, Tukuba, Japan

**Abstract.** On October 19, 1996, a large underthrusting earthquake ( $M_s = 6.7$ ), the Hyuga-nada, Japan, earthquake occurred along the southern end of Nankai trough. About two months later, a second large earthquake ( $M_s = 6.7$ ) occurred in the adjacent region. We study the source process of the two large earthquakes in the Hyuga-nada region and compare the coseismic rupture area with aftershock distribution. The main source parameters obtained for the first mainshock are: (strike, dip, rake) = (210°, 12°, 81°); the seismic moment  $M_o = 2.3 \times 10^{19}$  Nm ( $M_w = 6.8$ ); the rupture area  $S = 20 \times 15$  km<sup>2</sup>, and the source duration  $T = 17$  s. For the second main-shock, (strike, dip, rake) = (210°, 12°, 87°); the seismic moment  $M_o = 1.5 \times 10^{19}$  Nm ( $M_w = 6.7$ ); the rupture area  $S = 18 \times 18$  km<sup>2</sup>, and the source duration  $T = 15$  s. The coseismic rupture areas do not overlap the aftershock area, while the aftershock areas of the two main-shocks mutually overlap. This implies that the common aftershock region takes a role of barriers to dynamic rupture. It is also seen that the aftershock area expanded during the first one day.

## 1. Introduction

A large earthquake with  $M_s 6.7$  occurred on October 19, 1996 in the Hyuga-nada, Kyushu, Japan. About two months later, another large earthquake with  $M_s 6.7$  occurred in the adjacent region. The source information is given in Table 1. The cumulative number of earthquakes ( $M \geq 2$ ) from October 1st to December 31st in 1996 in Hyuga-nada region is given in Figure 1. Centroid moment tensors of both earthquakes are quite similar [Dziewonski *et al.*, 1998]. The aftershock distributions as well as the focal mechanism suggest that both earthquakes are low-angle thrust along the plate boundary between the Philippine Sea Plate and the Eurasian Plate.

In this paper, we derive the details of the rupture process of the above two earthquakes using near-field records and GPS displacement vectors, and examine the relationship between coseismic rupture area and aftershock area.

## 2. Data and Method

We retrieved acceleration data recorded at K-NET stations [National Research Institute for Earth Science and Disaster Prevention (NIED)] [Kinoshita, 1998]. 25 components at 11 stations were used to investigate the source rupture process of main-shocks. Strong motion seismograph stations used in our analysis are shown in Figure 2b. The acceleration data were numerically integrated and bandpassed between 0.05 and 0.4 Hz.

In addition to the seismic data, we also used GPS displacement data obtained by the continuous GPS network of Geographical Survey Institute [Tada *et al.*, 1997]. This continuous GPS displacement must consist of coseismic and

postseismic displacement caused by the Hyuga-nada earthquake [Nishimura *et al.*, 1999] and Tanegashima earthquake [Origin time: 10h50m24.3s, October 18, 1996 (GMT), epicenter: 30.630 N, 131.063 E, depth: 10.0km, Ms: 6.6 (USGS)]. We modeled the coseismic displacement as a step function and the postseismic displacement as an exponential function:  $[1 - \exp(-t/T)]$ , to determine the coseismic and the postseismic displacements by the least squares method.

We employed a multiple-time window inversion to determine the temporal and spatial distribution of fault slip. Then the constraint of smoothness and positivity were imposed on the solution. To determine the smoothness parameter objectively, we adopted the minimum Akaike's Bayesian information criterion (ABIC) [Akaike, 1980]. The minimum ABIC has been successfully applied to various inversion problems [e.g. Yoshida, 1989 and Yabuki and Matsu'ura, 1992]. Green's function was calculated by the discrete wave number method developed by Kohketsu [1985] with the underground structure obtained by Iwasaki *et al.* [1990] as shown in Table 2.

### 3. The Hyuga-nada earthquake of October 19

We assumed a single fault plane: (strike, dip) = (210°, 12°) which is inferred from the aftershock distribution, moment tensor solution [Dziewonski *et al.*, 1998] and the velocity structure by Ichikawa [1997]. A grid scheme was constructed on the fault plane so that it covered the aftershock area. An area of  $32.12 \times 32.12$  km<sup>2</sup> were divided into 121 subfaults, each having an area of  $2.92 \times 2.92$  km<sup>2</sup>. Fractional number of the grid spacing came from the continuation of the grid scheme to the hypocenter of the next main-shock. The slip-rate function of each subfault was expanded in a series of 8 triangle functions whose rise time is 0.8 s. The rake was allowed to vary within the range of  $80^\circ \pm 45^\circ$ . The total number of the model parameters is  $11 \times 11 \times 8 \times 2 = 1936$ . In addition we varied the hypocenter depth from 11 to 19 km with an increment of 4 km and the maximum rupture front velocity ( $V_{\text{max}}$ ) from 1.8 to 3.0 km/s. In order to determine the relative weight between K-NET data and GPS data, we assumed the standard deviation of the K-NET data as 20% of the maximum amplitude and the standard deviation of GPS data as 0.5 cm.

The minimum variance was found for hypocenter depth = 15 km and  $V_{\text{max}} = 2.2$  km/s. The hypocenter depth is consistent with the plate boundary obtained by the ocean bottom seismographic surveys [Ichikawa, 1997]. Figure 2 displays a comparison of the observed records (black) with the synthetics (red). The waveform fit seems rather good. The difference of a factor of 2 may be accounted for by a local structure effect. Figure 3 represents the spatial distribution of the coseismic slip and the moment rate function obtained in this study. The total seismic moment is  $2.3 \times 10^{19}$  Nm and the duration of moment release is 17 s. A large slip occurs about 3 km west from the hypocenter, where the maximum slip is about 2.9 m. The fault area is  $20 \times 15$  km<sup>2</sup>. The average rake is  $81^\circ$ , which is consistent with the moment tensor solution [Dziewonski *et al.*, 1998].

The aftershock activity seems to be low in the asperity where large slip occurred, and very high at southern portion outside the asperity. The aftershock area amounts to about  $35 \times 30$  km<sup>2</sup> which is significantly larger than the coseismic rupture area.

#### 4. The Hyuga-nada earthquake of December 2

We used the same fault strike as the first main-shock. The dip angle of the fault plane is not well constrained by the plate boundary structure found in the literatures [e.g. *Ichikawa, 1997*] nor by the aftershock distribution. Therefore, we tried to determine the dip angle in inversion procedure.

In order to obtain a gross feature as well as some detail of the rupture process, we divided the procedure into two steps. At the first step, we took a broad fault area of  $30 \times 36 \text{ km}^2$  to determine the dip angle, hypocenter depth,  $V_{\text{rmax}}$  and a rough estimation of rupture area. The area was divided into 30 subfaults, each having an area of  $6 \times 6 \text{ km}^2$ . The slip-rate function of each subfault was expanded in a series of 3 triangle functions whose rise time is 1.6 s. The minimum variance was found for dip angle =  $12^\circ$ , depth = 21 km and  $V_{\text{rmax}} = 2.0 \text{ km/s}$ . A major slip took place in an area of  $12 \times 18 \text{ km}^2$ . At the second step, we fixed the dip angle, hypocenter depth and  $V_{\text{rmax}}$ . The fault plane was then confined to  $29.2 \times 29.2 \text{ km}^2$  and divided into 100 subfaults, each having an area of  $2.92 \times 2.92 \text{ km}^2$ . The slip-rate function of each subfault is expanded in a series of 6 triangle functions with a rise time of 0.8 s. The number of the model parameters is  $10 \times 10 \times 6 \times 2 = 1200$ . We assumed the same standard deviations of K-NET data and GPS data as that of the first main-shock.

Figure 4 displays a comparison of the observed records with the synthetics. The waveform fit seems rather good. Figure 5 represents a spatial distribution of the coseismic slip and the moment rate function obtained by the joint inversion. The total seismic moment is  $1.5 \times 10^{19} \text{ Nm}$ . The duration of moment release is 15 s. The asperity is located at about 10 km northeast from the epicenter, where the maximum slip is about 1.4 m. The coseismic rupture area is  $18 \times 18 \text{ km}^2$ . The average rake is  $87^\circ$  which is consistent with the moment tensor solution [*Dziwowski et al., 1998*]. The aftershock area is about  $20 \times 30 \text{ km}^2$ .

The slip distribution and the aftershock area for both main-shocks are summarized in Figure 6. It is interesting to note that this aftershock area does not overlap the coseismic rupture area, but does the aftershock area of the first main-shock. Moreover, the aftershock area expanded rapidly during the first one day after the main-shock (Figures 3 and 5). The similar phenomenon is reported by *Tajima and Kanamori [1985]* and *Wesson [1987]*.

#### 5. Discussion

Coseismic rupture area is often estimated from aftershock area. However, recent studies on the details of moment release distribution show that aftershocks tend to expand into a surrounding area of the coseismic slip region [*Mendoza and Hartzell, 1988, Takeo and Mikami, 1990, Ide and Takeo, 1996*]. Our results also show a similar tendency. These observations suggest that the aftershock area is not necessarily a good indicator of the coseismic rupture area.

As shown in the Hyuga-nada events, the aftershock area of the first main-shock was partly re-activated by the second main-shock. It is very remarkable that re-activated aftershock area was almost free from coseismic moment release. This implies that the common aftershock area took a part of barriers to dynamic rupture in both main-shocks. A similar evidence is observed in the aftershock distribution of the 1996 Andreanof Islands earthquake. A part of the aftershock area of the 1986 Andreanof Islands earthquake was re-activated by the 1996 Andreanof Islands earthquake [*Kisslinger and Kikuchi, 1997*]. It is interesting to note that this aftershock

area had a role of barriers to dynamic rupture at the 1986 Andreanof Islands earthquake [Yoshida, 1992], and the area had little coseismic moment release at the 1996 Andreanof Islands earthquake [Kisslinger and Kikuchi, 1997].

Another interesting evidence is that the aftershock area expanded rapidly during the first one day (Figure 6). The expansion of aftershock area was prominent especially in the common aftershock area. Those suggest that a quasi-static rupture and/or deformation propagated in the aftershock area as proposed by Scholz [1990] and Wesson [1987].

**Acknowledgments.** The earthquake hypocenters used in this paper were taken from the web of the Shimabara Earthquake and Volcano Observatory Faculty of Science, Kyushu University. K. Uehira of Kyushu University provided estimation error of location of hypocenter. This work was partly supported by the Grant-in-Aid for Scientific Research No. 10640399, from the Ministry of Education, Japan.

## References

- Akaike, H., Likelihood and the Bayes procedure, in *Bayesian Statistics*, edited by J. M. Bernardo, M. H. DeGroot, D. V. Lindley, and A. F. M. Smith, pp. 143-166, University Press, Valencia, Spain, 1980.
- Dziewonski, A. M., G. Ekström, N. N. Maternovskaya, Centroid-moment tensor solution for October-December, 1996, *Phys. Earth Planet. Interiors*, *105*, 95-108, 1998.
- Ichikawa, G., Ocean Bottom Seismographic Experiment to Study Crustal Structure in Hyuga-nada, *M. Sc. Thesis, University of Hokkaido* (in Japanese), 1997.
- Ide, S. and M. Takeo, The dynamic rupture process of the 1993 Kushiro-oki earthquake, *J. Geophys. Res.*, *101*, 5661-5675, 1996.
- Iwasaki, T., N. Hirata, T. Kanazawa, J. Melles, K. Suyehiro, T. Urabe, L. Möller, J. Makris and H. Shimamura, Crustal and upper mantle structure in the Ryukyu Island Arc deduced from deep seismic sounding, *Geophys. J. Int.*, *102*, 631-651, 1990.
- Kinoshita, S., Kyoshin Net (K-NET), *Seismological Research Letters*, *69*, 1998.
- Kisslinger, C., and M. Kikuchi, Aftershocks of the Andean Islands earthquake of June 10, 1996, and local seismotectonics, *Geophys. Res. Letters*, *24*, 1883-1886, 1997.
- Kohketsu, K., The extended reflectivity method for synthetic near-field seismograms, *J. Phys. Earth*, *33*, 121-131, 1985.
- Mendoza, C. and S. H. Hartzell, Aftershock patterns and main shock faulting, *Bull. Seism. Soc. Am.*, *78*, 1438-1449, 1988.
- Nishimura, S., M. Ando and S. Miyazaki, Inter-plate Coupling Along the Nankai Trough and Southeastward Motion Along Southern Part of Kyushu, *Zishin* (in Japanese), *2*, *51*, 443-456, 1999.
- Scholz, C. H., *The Mechanics of Earthquake and Faulting*, 321pp., Cambridge University Press, New York, 1990.
- Tada, T., T. Sagiya and S. Miyazaki, Crustal deformation in the Japan Islands by using GPS network, *Kagaku* (in Japanese), *67*, 917-927, 1997.
- Tajima, F. and H. Kanamori, Global survey of aftershock area expansion patterns, *Phys. Earth Planet. Inter.*, *40*, 77-134, 1985.
- Takeo, M. and N. Mikami, Fault heterogeneity of inland earthquake in Japan, *Bull. Earthquake Res. Inst. Univ. Tokyo*, *65*, 541-569, 1990.
- Yabuki, T. and M. Mats'ura, Geodetic data inversion using a Bayesian information criterion for spatial distribution of fault slip, *Geophys. J. Int.*, *109*, 363-375, 1992.
- Yoshida, S., Waveform inversion using ABIC for the rupture process of the 1983 Hindu Kush earthquake, *Phys. Earth Planet. Interiors*, *56*, 389 - 405, 1989.
- Yoshida, Waveform inversion for rupture process using a non-flat seafloor model: application to 1986 Andean Islands and 1985 Chile earthquakes, *Tectonophysics*, *211*, 45-59, 1992.
- Wesson, R., Modeling aftershock migration and afterslip of the San Juan Bautista, California, earthquake of October 3, 1973, *Tectonophysics*, *144*, 215-229, 1987.

Y. Yagi, M. Kikuchi and S. Yoshida, Earthquake Research Institute, The University of Tokyo, 1-1-1, Yayoi, Bunkyo-ku, Tokyo, 113-0032, Japan. (e-mail: yuji@eri.u-tokyo.ac.jp, kikuchi@eri.u-tokyo.ac.jp and shingo@eri.u-tokyo.ac.jp)

T. Sagiya, Geographical Survey Institute, 1, Kitago, Tsukuba, 305-0811, Japan. (e-mail: sagiya@gsi-mc.go.jp)

(Received January 22, 1999; revised June 25, 1999; accepted July 20, 1999.)

YAGI ET AL.: COSEISMIC RUPTURE AND AFTERSHOCKS

YAGI ET AL.: COSEISMIC RUPTURE AND AFTERSHOCKS

YAGI ET AL.: COSEISMIC RUPTURE AND AFTERSHOCKS

**Figure 1.** The Cumulative number of earthquakes (M 2) from October 1st to December 31st in 1996 in Hyuga-nada region [Shimabara Earthquake Volcano Observatory, Faculty of Science, Kyushu University].

**Figure 2.** Comparison of the observations (black) with the calculations (red) for the October 19, 1996 Hyuga-nada earthquake. a) velocity waveforms at some representative

stations, b) horizontal GPS displacements. The station location of strong motion records used in our analysis are shown by blue triangles.

**Figure 3.** Comparison between the foreshock (orange diamonds), the one-hour aftershock (violet circles), the one-day aftershock (blue circles), and the coseismic fault slip for the October 19, 1996 Hyuga-nada earthquake. The rectangle represents the area of the subfaults assumed in the inversion. The estimation error of location is shown by cross bar. The inset shows the moment-rate function.

**Figure 4.** Comparison of the observations (black) with the calculations (red) for the December 2, 1996 Hyuga-nada earthquake. a) velocity waveforms, b) horizontal GPS displacements.

**Figure 5.** The coseismic fault slip, one-hour aftershock (violet squares) and one-day aftershocks (blue squares) for the December 2, Hyuga-nada earthquake. The rectangle represents the area of the subfaults assumed in the inversion (dashed and solid lines represent large and detailed fault models, respectively). The estimation error of location is shown by cross bar. The inset shows the moment-rate function.

**Figure 6.** Map view of the one-day aftershock for the first main-shock (blue circles) and for the second main-shock (red diamonds). Contours show the slip pattern determined in this study. The contour interval is 0.5m.

**Table 1.** Source information of two main-shocks determined by Kyushu University.

Date	Time	Latitude	Longitude	Depth (km)	Ms*
October 19, 1996	14:44:41.9	31.835 ° N	131.958 ° E	11.6	6.7
December 2, 1996	22:17:59.5	31.803 ° N	131.588 ° E	20.4	6.7

\* Ms determined by USGS

**Table 2.** Velocity Structure in Hyuga-nada region..

H km	Vp km/s	Vs km/s	$\rho$ , $\times 10^3$ kg/m <sup>3</sup>	Qp	Qs
1.5	3.5	2.0	2.3	300	150
8	5.6	3.2	2.6	400	200
15	6.0	3.5	2.8	500	250
24	6.6	3.8	3.0	800	400
30	6.8	3.9	3.0	800	400
	7.8	4.5	3.2	1000	500

Figure 1

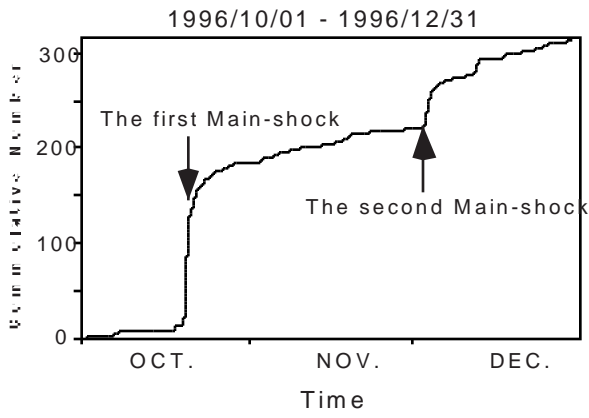


Figure 2

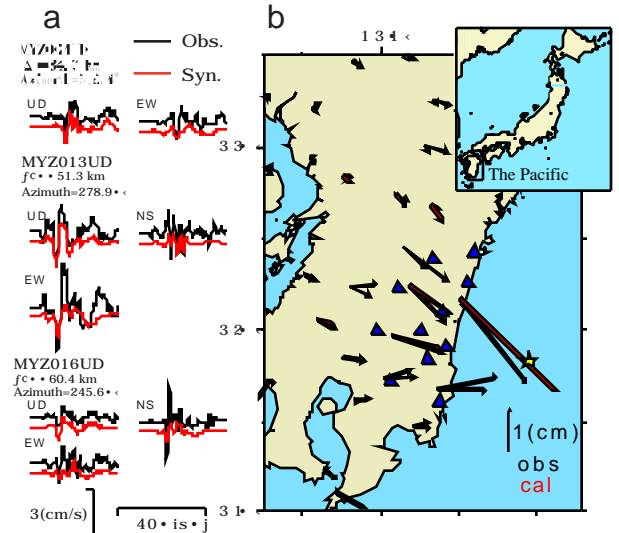


Figure 3

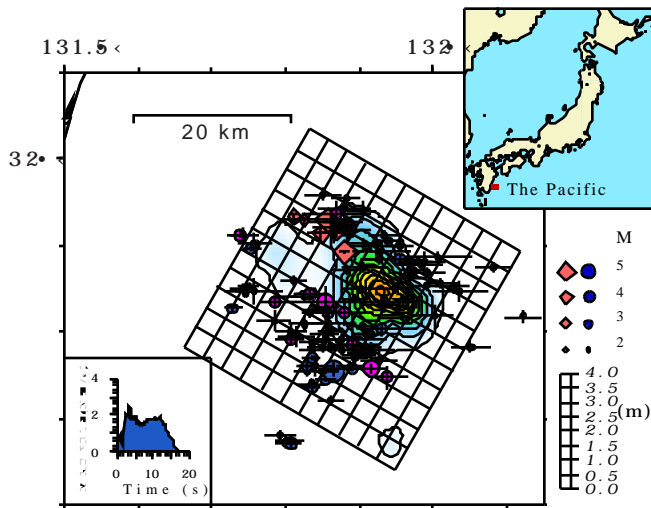


Figure 4

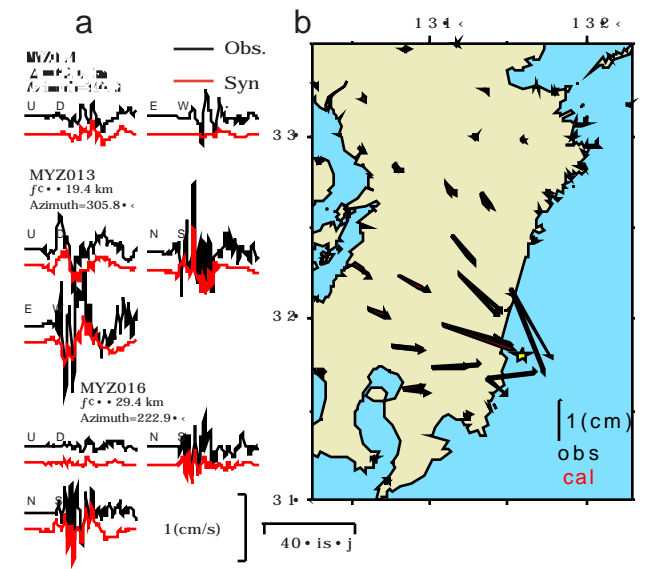


Figure 5

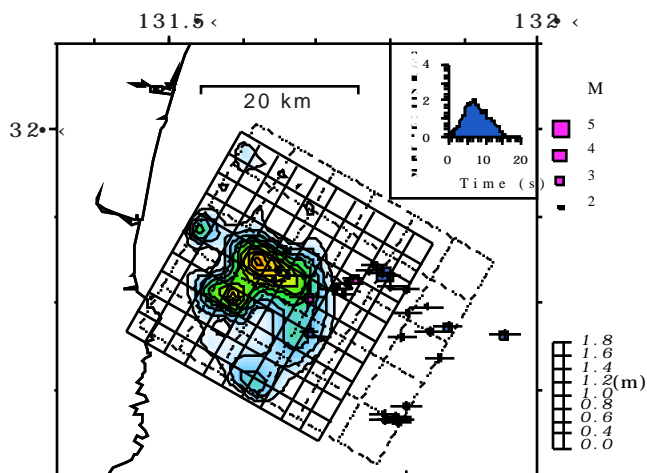


Figure 6

